

Original Research



Sanghuangporus sanghuang extract inhibits the proliferation and invasion of lung cancer cells *in vitro* and *in vivo*

Weike Wang ¹, Jiling Song ¹, Na Lu ¹, Jing Yan ¹, and Guanping Chen ^{2§}

¹Institute of Vegetable Science, Hangzhou Academy of Agricultural Sciences, Hangzhou 310024, China

²Cancer Institute of Integrated Traditional Chinese and Western Medicine, Zhejiang Academy of Traditional Chinese Medicine, Tongde Hospital of Zhejiang Province, Hangzhou 310012, China

OPEN ACCESS

Received: May 1, 2023

Revised: Sep 1, 2023

Accepted: Oct 23, 2023

Published online: Nov 8, 2023

§Corresponding Author:

Guanping Chen


Cancer Institute of Integrated Traditional Chinese and Western Medicine, Zhejiang Academy of Traditional Chinese Medicine, Tongde Hospital of Zhejiang Province, 234 Gucui Road, Hangzhou 310012, China.
Tel. +86-571-88849085
Fax. +86-571-88849085
Email. beyond_cgcp@163.com

©2023 The Korean Nutrition Society and the Korean Society of Community Nutrition
This is an Open Access article distributed under the terms of the Creative Commons Attribution Non-Commercial License (<https://creativecommons.org/licenses/by-nc/4.0/>) which permits unrestricted non-commercial use, distribution, and reproduction in any medium, provided the original work is properly cited.

ORCID iDs

Weike Wang 


<https://orcid.org/0000-0002-2228-6519>

Jiling Song 


<https://orcid.org/0000-0003-4858-4319>

Na Lu 

<https://orcid.org/0000-0002-9635-9020>

Jing Yan 

<https://orcid.org/0000-0001-5116-9293>

Guanping Chen 

<https://orcid.org/0000-0002-2229-9424>

Funding

This work was supported by the Zhejiang Province Public Welfare Technology

ABSTRACT

BACKGROUND/OBJECTIVES: *Sanghuangporus sanghuang* (SS) has various medicinal effects, including anti-inflammation and anticancer activities. Despite the extensive research on SS, its molecular mechanisms of action on lung cancer are unclear. This study examined the impact of an SS alcohol extract (SAE) on lung cancer using *in vitro* and *in vivo* models.

MATERIALS/METHODS: Different concentrations of SAE were used to culture lung cancer cells (A549 and H1650). A cell counting kit-8 assay was used to detect the survival ability of A549 and H1650 cells. A scratch assay and transwell cell invasion assay were used to detect the migration rate and invasive ability of SAE. Western blot analysis was used to detect the expression of B-cell lymphoma-2 (Bcl-2), Bcl2-associated X (Bax), cyclin D1, cyclin-dependent kinases 4 (CDK4), signal transducer and activator of transcription 3 (STAT3), and phosphorylated STAT3 (p-STAT3). Lung cancer xenograft mice were used to detect the inhibiting ability of SAE *in vivo*. Hematoxylin and eosin staining and immunohistochemistry were used to detect the effect of SAE on the structural changes to the tumor and the expression of Bcl-2, Bax, cyclin D1, CDK4, STAT3, and p-STAT3 in lung cancer xenograft mice.

RESULTS: SAE could inhibit lung cancer proliferation significantly *in vitro* and *in vivo* without cytotoxicity. SAE suppressed the viability, migration, and invasion of lung cancer cells in a dose and time-dependent manner. The SAE treatment significantly decreased the proapoptotic Bcl-2/Bax ratio and the expression of pro-proliferative proteins Cyclin D1 and CDK4 *in vitro* and *in vivo*. Furthermore, SAE also inhibited STAT3 expression.

CONCLUSIONS: SAE reduced the cell viability and suppressed cell migration and invasion in human lung cancer cells. Moreover, SAE also exhibited anti-proliferation effects *in vivo*. Therefore, SAE may have benefits in cancer therapy.

Keywords: *Sanghuangporus sanghuang*; plant extracts; cell proliferation; neoplasm invasion; non-small cell lung cancer

INTRODUCTION

Lung cancer is the leading cause of cancer-related death worldwide. Non-small cell lung cancer (NSCLC) comprises more than 85% of primary lung cancers. The long-range survival of sufferers remains poor; approximately 40–50% of patients with NSCLC present with an advanced stage [1,2]. Despite the significant progress in the diagnosis and medication of

Application Research Project (No. LTGD23C040004) and the Hangzhou Scientific and Technological Commission (No. 20180416A02).

Conflict of Interest

The authors declare no potential conflicts of interests.

Author Contributions

Data curation: Wang W, Song J; Formal analysis: Wang W, Yan J; Funding acquisition: Chen G; Investigation: Wang W; Methodology: Chen G; Software: Lu N; Validation: Lu N; Visualization: Song J; Writing - original draft: Chen G; Writing - review & editing: Wang W.

lung adenocarcinoma in recent years, the 5-yr survival rate of NSCLC is still low [3]. Systemic chemotherapy is the recommended treatment strategy for lung cancer patients. On the other hand, traditional chemotherapy causes systemic toxicity and drug resistance, which narrows its effect and may be the leading cause of chemotherapy failure [4,5]. Therefore, the discovery and development of new drugs with low toxicity remains a challenge in the treatment of NSCLC.

Traditional Chinese medicine (TCM) is widely accepted in many medical contexts, particularly treating cancers [6]. Evidence in preclinical and clinical trials has shown that herbs or medicinal plants could improve the efficacy of chemotherapy, reduce toxicity, enhance the immune function, prevent metastasis, and improve the quality of life of patients [7]. *Sanghuangporus sanghuang* (SS) is a popular pharmacodynamic and economically important edible fungus that grows on the trunk of mulberry trees [8]. The sanghuang strain and its extracts have been reported to exhibit immune strengthening, antioxidant, anti-inflammatory, and antitumor activities [9]. SS can inhibit the proliferation of human colon cancer cells [10], prostate cancer cells [11], and breast cancer cells [12]. Nevertheless, the effects of the SS alcohol extract (SAE) on human lung cancer cells are unclear. This study examined the effect of SAE on human lung cancer cells and its potential molecular mechanism both *in vitro* and *in vivo*.

MATERIALS AND METHODS

Materials

RPMI 1640 medium and penicillin/streptomycin were purchased from Gibco (Grand Island, NY, USA); fetal bovine serum (FBS) was obtained from HyClone (Logan, UT, USA); 5-ethynyl-2'-deoxyuridine (EdU) and cell counting kit-8 (CCK-8) were acquired from MedChemExpress (Monmouth Junction, NJ, USA); the bicinchoninic acid (BCA) protein assay kit was supplied by Pierce (Rockford, IL, USA); the polyvinylidene difluoride (PVDF) membrane was procured from Roche (Indianapolis, IN, USA); Matrigel was purchased from Sigma-Aldrich (St. Louis, MO, USA); the antibodies against B-cell lymphoma-2 (Bcl-2, 26 kDa; Cat. No. 3498), cyclin D1 (36 kDa; Cat. No. 55506), Bcl2-associated X (Bax, 20 kDa; Cat. No. 14796), cyclin-dependent kinases 4 (CDK4, 30 kDa; Cat. No. 12790), signal transducer and activator of transcription 3 (STAT3, 79,86 kDa; Cat. No. 12640), phosphorylated STAT3 (p-STAT3, 79,86 kDa; Cat. No. 9145), glyceraldehyde 3-phosphate dehydrogenase (GAPDH, 133 kDa; Cat. No. 2118) were supplied by Cell Signaling Technology (Boston, MA, USA).

Preparation of SAE

SS was authenticated by the Institute of Microbiology, Chinese Academy of Sciences, Beijing, China. The fruiting body powder (150 g) was extracted three times with 80% (V/V) ethanol for two hours each at room temperature. Three extractions were combined, evaporated at 40°C, and freeze-dried for 72 h. The powder was dissolved in dimethyl sulfoxide and centrifuged at 12,000 rpm for 5 min at 4°C to make a final concentration of 200 mg/mL. The supernatant SAE was stored at -80°C until further use.

Cell culture

The human non-small cell lung cancer cells A549 and NCI-H1650 were obtained from the Cell Bank of the Chinese Academy of Sciences. The cells were cultured in RPMI 1640 medium supplemented with 10% FBS and 1% penicillin/streptomycin at 37°C in a humidified 5% CO₂ atmosphere (Thermo Fisher Scientific, Waltham, MA, USA).

Cell viability analysis

Logarithmic growth phase A549 and H1650 cells were selected, and the cell concentration was adjusted to 3.5×10^4 /mL with the full medium, and 0.1 mL was added to each well of a 96-well plate. After culturing for 24 h, the medium was discarded, and 0, 3, 6, or 9 mg/mL SAE medium was added, respectively. After culturing for 12, 24, or 48 h, the cells were taken out, and 10 μ L CCK-8 was added to each well and then incubated for 3 h at 37°C. The optical density values were measured at 450 nm using a microplate reader (Molecular Devices, San Jose, CA, USA).

Cell proliferation assay

Cell proliferation was evaluated by treating A549 and H1650 cells with the indicated concentrations of SAE (0, 3, 6, or 9 mg/mL) for 48 h. The cells were assayed using the EdU Imaging Kit according to the manufacturer's instructions and counterstained with Hoechst 33342 (Abcam, Cambridge, UK). The percentage of proliferation cells per slide in 5 random fields of view was determined using an inverted fluorescence microscope (Olympus, Tokyo, Japan).

Cell migration assay

The wound healing assay was used to evaluate the ability of cell migration. When the cells were grown to 80% confluence in 6-well plates, wounds were produced by scratching the confluent cell monolayer using a 200 μ L pipette tip. The cells were then washed three times with phosphate-buffered saline (PBS) to remove the scratched cells and incubated with the medium containing 0 mg/mL, 3 mg/mL, 6 mg/mL, or 9 mg/mL SAE for 48 h. The width of the scratch was photographed at 0 and 24 h under a microscope (Olympus).

Cell invasion assay

Cell invasion was determined using a BD 24-Transwell plate with 8 μ m membranes according to the manufacturer's instructions (BD, Franklin Lakes, NJ, USA). Approximately 1×10^5 cells suspended in 200 μ L serum-free RPMI 1640 medium (Gibco) containing different concentrations of SAE (0, 3, 6, or 9 mg/mL) were added to the upper chamber, and 0.75 mL of RPMI 1640 with 10% FBS was added to the lower chamber. After incubation for 24 h, the invading cells in five microscope areas were counted and imaged by a microscope (Olympus).

Western blotting analysis

The A549 and H1650 cells were seeded (1×10^5 cells/well) in a six-well plate, treated with RPMI 1640 containing SAE at concentrations of 0, 3, 6, or 9 mg/mL, and cultured for 24 h at 37°C. The cells were scraped at the end of treatments and lysed in radioimmunoprecipitation assay buffer (Solarbio, Wuhan, China) containing a protease inhibitor and phosphatase inhibitor for 15 min on ice. The protein concentration was calculated using a BCA protein assay kit. A 30 μ g sample of protein was resolved into 12% sodium dodecyl sulfate-polyacrylamide gel electrophoresis and transferred to a PVDF membrane. The membrane was incubated overnight with the monoclonal antibodies against Bcl-2, Bax, cyclin D1, CDK4, STAT3, p-STAT3, and GAPDH in a blocking buffer at 4°C. Horseradish peroxidase (HRP)-conjugated anti-IgG was used as a secondary antibody at room temperature for 1 h. A chemiluminescence system was used to visualize the immune complexes, and the band optical densities were quantified against the GAPDH band using Image J Version 1.8.0 software (NIH, Bethesda, MD, USA).

Animal experiment

Male BALB/c nude mice (initial body weight about 16–18 g) were obtained from Beijing Vital River Laboratory Animal Technologies Co. Ltd. and housed under SPF conditions with a controlled temperature (range: 18–22°C), humidity (30–60%), and a 12 h light/dark cycle. The A549 cells were grown in culture and detached by trypsinization. Approximately 1.0×10^6 cells mixed with Matrigel (1:1) were injected subcutaneously into the right flank area of nude mice to initiate tumor growth. Seven days after implantation, the mice were randomized into two groups ($n = 6$ /group). The control group was administered normal saline, while the treatment group received daily intraperitoneal (IP) injections of 40 mg/kg SAE. The body weight was measured daily to evaluate the adverse effects of SAE on mice. The tumor volume was determined using the formula $(L \times W^2)/2$, where L is the diameter of the longest dimension, and W is the orthogonal diameter. At the end of the experiment, the animals were euthanized by cervical dislocation, and the tumor tissue was removed and weighed. The tumor was fixed in buffered formalin for hematoxylin and eosin (HE) staining and immunohistochemistry (IHC) analyses.

Histological examination by HE staining

The tumors were fixed with 10% buffered formalin for 24 h and embedded in paraffin. Subsequently, 4 μ m sections were cut, deparaffinized, and rehydrated. The sections were then stained with HE. The histopathological changes were observed under an optical microscope (Leica, Weztlar, Germany).

IHC assay

Paraffin-embedded samples were sectioned and washed with PBS, microwaved in citrate buffer to unmask the antigens, and the slides were then incubated with rabbit monoclonal antibodies against Bcl-2, Bax, CyclinD1, CDK4, STAT3, and p-STAT3 (all in 1:200 dilution). After washing, the slides were incubated with biotinylated secondary antibody followed by HRP-conjugated streptavidin and washed. The slides were then incubated with diaminobenzidine as the chromogen, followed by counterstaining with diluted Harris Hematoxylin. After staining, 5 high-power fields (200 \times) were selected randomly in each slide. The average proportion of positive cells in each field was counted using Image J (NIH).

Statistical analysis

All analyses were conducted using SPSS 17.0 for Windows (SPSS, Chicago, IL, USA). The data are presented as the mean \pm standard deviation (SD). The statistical significance of the difference between the SAE and control was assessed using a Student's *t*-test. The significant differences among three or more groups were evaluated using a one-way analysis of variance test, followed by a Bonferroni test. Differences with *P*-values < 0.05 were considered significant.

RESULTS

SAE inhibit the proliferation of A549 and H1650 cells

Cell viability analysis showed that SAE could inhibit the proliferation and DNA synthesis of A549 and H1650 cells in a dose and time-dependent manner. After being treated with SAE for 12 h, cell proliferation and cell DNA synthesis of the 3 mg/mL group did not decrease significantly compared to the control group. On the other hand, there was a significant decrease in the 9 mg/mL group compared to the control group. The cell proliferation (**Fig. 1A and B**) and DNA synthesis (**Fig. 1C and D**) decreased significantly in all treatment groups compared to the control group after treatment for 48 h.

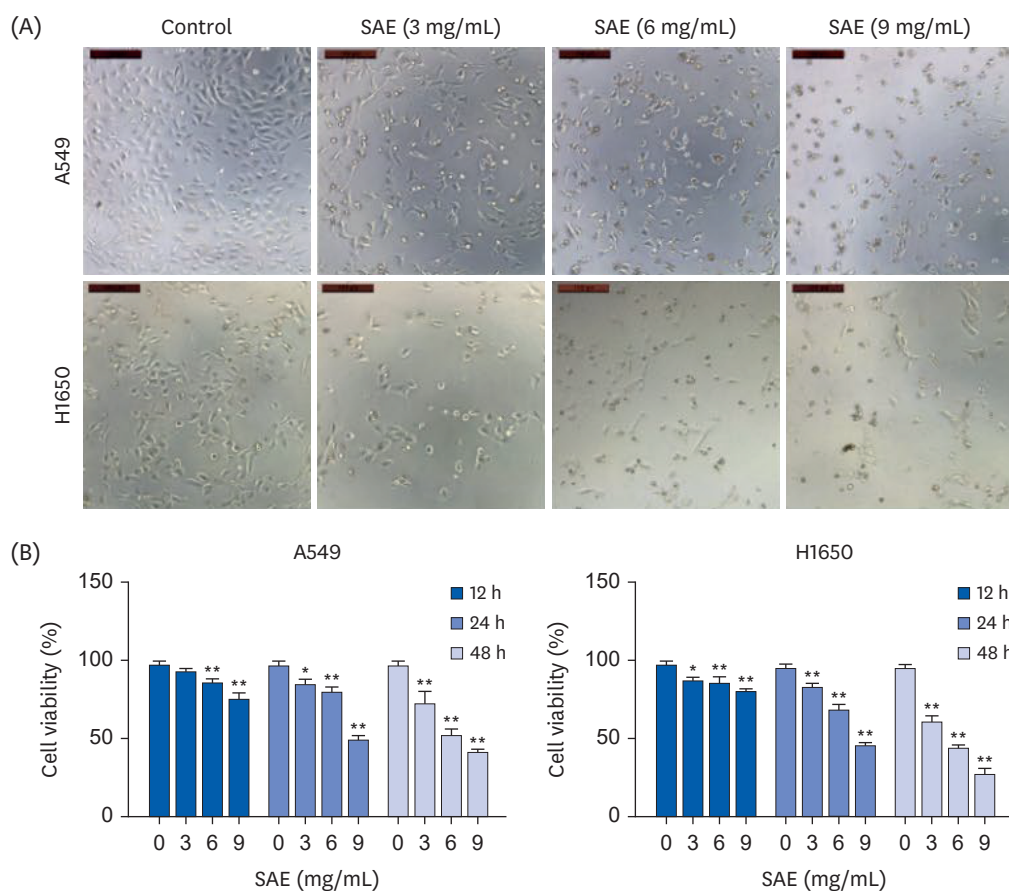


Fig. 1. SAE significantly suppresses the proliferation and DNA synthesis of lung cancer cells. (A) The morphology of A549 and H1650 cells treated with SAE at the concentrations of 0, 3, 6 and 9 mg/mL for 48 h were observed. Representative images are presented (200 \times). (B) The viability of A549 and H1650 cells were inhibited by SAE in a dose and time-dependent manner. (C) EdU staining of lung cancer cells treated with various concentrations of SAE for 40 h. (D) Relative EdU-positive cell ratios for lung cancer cells treated with indicated concentration of SAE. SAE, *Sanghuangporus sanghuang* alcohol extract; EdU, 5-ethynyl-2'-deoxyuridine. * $P < 0.05$, ** $P < 0.01$ vs. untreated control.

(continued to the next page)

SAE inhibits the migration of A549 and H1650 cells

The scratch test results showed that the migration distances of A549 and H1650 cells decreased as the SAE concentration increased. In A549 cells, the migration distances of the 3 and 6 mg/mL groups after treatment for 24 h were $154.9 \pm 12.1 \mu\text{m}$ and $37.2 \pm 32.5 \mu\text{m}$, respectively, while the migration distance of the 9 mg/mL group after treatment for 24 h was $12.9 \pm 16.1 \mu\text{m}$. In the H1650 cells, the migration distances of the 3 and 6 mg/mL groups after treatment for 24 h were $385.7 \pm 34.3 \mu\text{m}$ and $196.3 \pm 43.7 \mu\text{m}$, respectively, while the migration distance of the 9 mg/mL group after treatment for 24 h was $124.6 \pm 29.4 \mu\text{m}$ (**Fig. 2**).

SAE inhibit the invasion of A549 and H1650 cells

Transwell showed that SAE inhibited the migration of A549 and H1650 cells in a dose-dependent. In A549 cells, the number of cells that passed through the filter membrane in the control group was 254.3 ± 13.6 after 24 h treatment. In contrast, the numbers were 62.7 ± 8.7 and 47 ± 6.4 in 6 and 9 mg/mL groups, respectively, suggesting that SAE could effectively inhibit the invasion of A549 cells. In H1650 cells, the number of cells that passed through the filter membrane in the control group after treatment for 24 h was 260.3 ± 16.7 , while there were 56.7 ± 1.3 and 49.2 ± 4.8 in the 6 and 9 mg/mL groups, respectively. Hence, SAE could also inhibit the invasion of H1650 cells (**Fig. 3**).

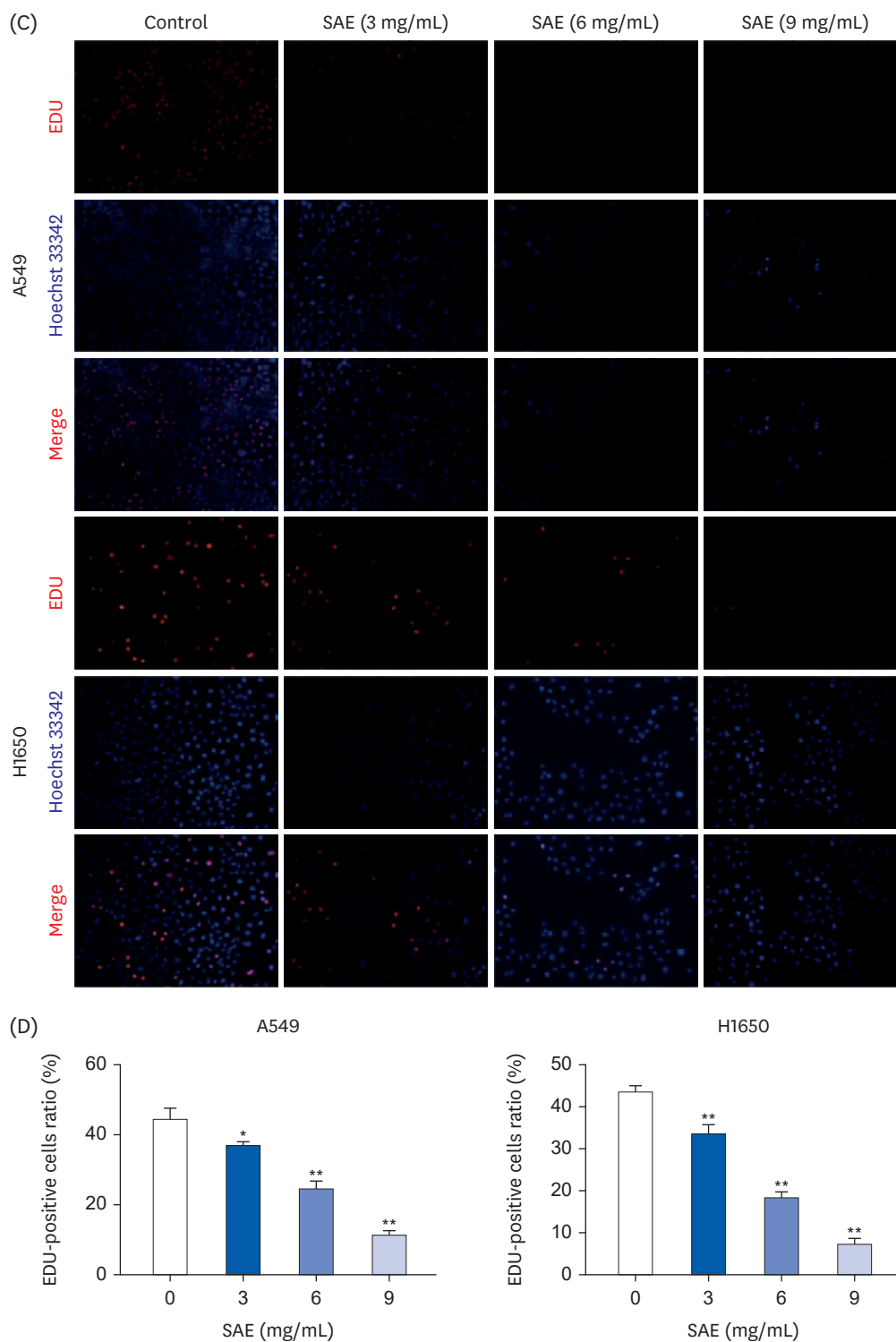


Fig. 1. (Continued) SAE significantly suppress the proliferation and DNA synthesis of lung cancer cells. (A) The morphology of A549 and H1650 cells treated with SAE at the concentrations of 0, 3, 6 and 9 mg/mL for 48 h were observed. Representative images are presented (200×). (B) The viability of A549 and H1650 cells were inhibited by SAE in a dose and time-dependent manner. (C) EdU staining of lung cancer cells treated with various concentrations of SAE for 40 h. (D) Relative EdU-positive cell ratios for lung cancer cells treated with indicated concentration of SAE.

SAE, *Sanghuangporus sanghuang* alcohol extract; EdU, 5-ethynyl-2'-deoxyuridine.

* $P < 0.05$, ** $P < 0.01$ vs. untreated control.

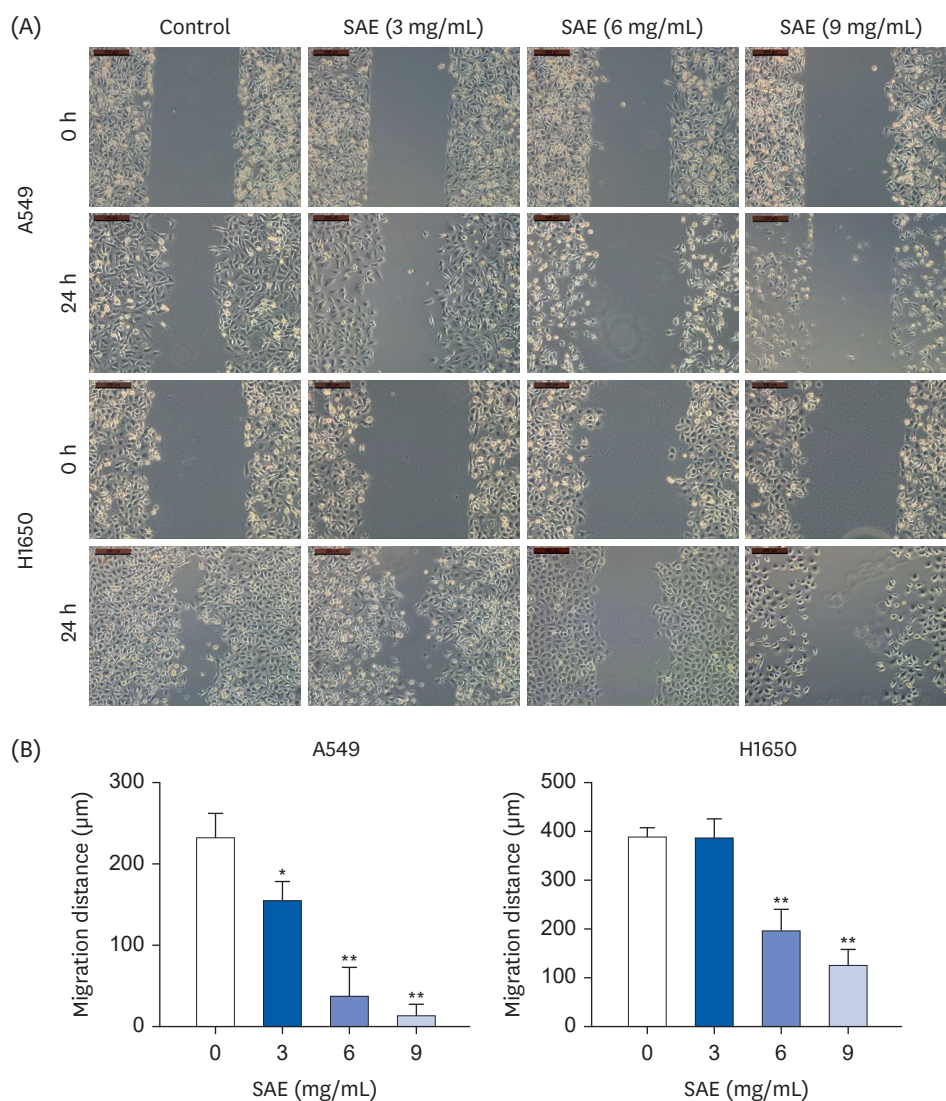


Fig. 2. SAE inhibit the migration of A549 and H1650 cells with the increased dose. (A) Effect of SAE on migration of lung cancer cell were assessed by scratch assay. The wound area were measured at 24 after treatment. Scale bar: 200 µm. (B) The data were calculated from 3 independent experiments and the results show the distance of the migration.

SAE, *Sanghuangporus sanghuang* alcohol extract.

* $P < 0.05$, ** $P < 0.01$ vs. untreated control.

SAE inhibited the STAT3 signaling pathway in A549 and H1650 cells

Western blotting results showed that SAE could down-regulate the expression levels of p-STAT3 in A549 and H1650 cells (Fig. 4A and B), suggesting that SAE inhibited the STAT3 signaling pathway in lung cancer cells. The levels of Bcl-2, CDK4, and Cyclin D1 expression in A549 and H1650 cells were also down regulated after the SAE treatment, and Bax expression was increased in the A549 and H1650 cells after the SAE treatment (Fig. 4C and D).

SAE inhibits the growth of lung cancer *in vivo*

The antitumor activity of SAE *in vivo* was determined by examining the tumor weight and volume in A549 xenograft mice, and its adverse effect was evaluated by measuring the changes in body weight. As shown in Fig. 5A and B, the SAE treatment reduced the tumor volume and weight significantly compared to the control. On the other hand, the

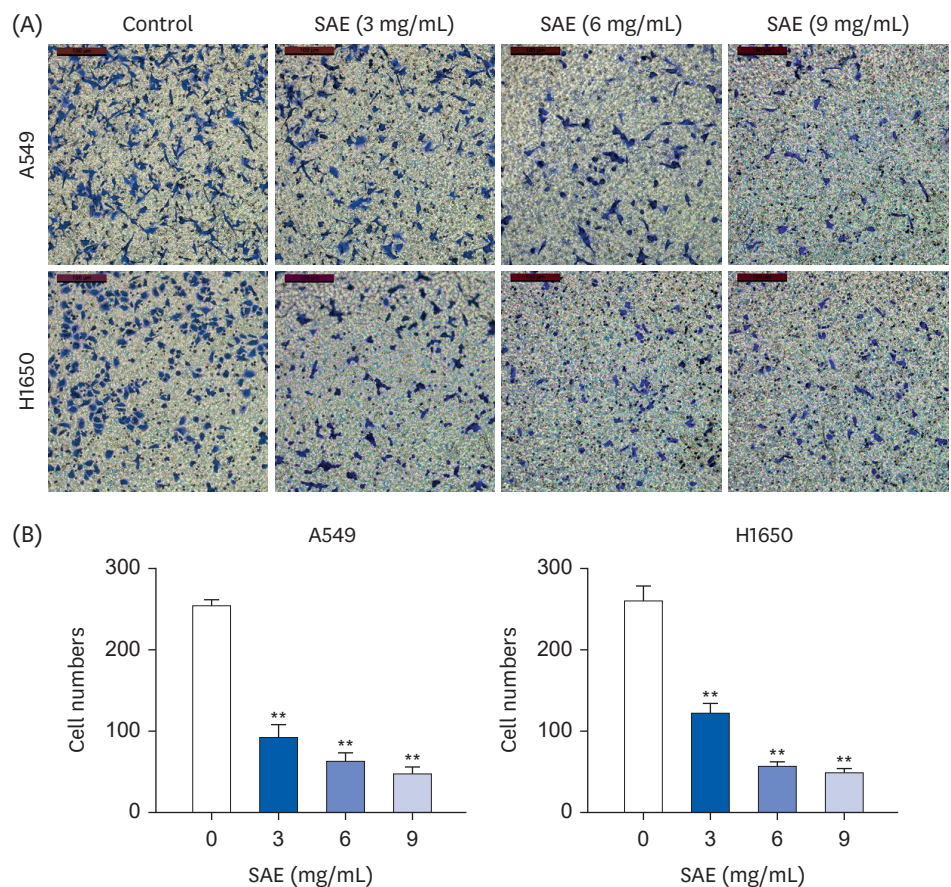


Fig. 3. SAE inhibit the invasion of A549 and H1650 cells in transwell assay. (A) Effect of SAE on invasion of lung cancer cell were assessed by transwell assay. (B) Transwell results showed that SAE inhibited cell invasion of A549 and H1650 in a dose-dependent manner. Magnification 200 \times . SAE, *Sanghuangporus sanghuang* alcohol extract. ** $P < 0.01$ vs. untreated control.

SAE treatment did not affect the changes in body weight (**Fig. 5D**). Thus, SAE effectively suppresses lung cancer growth in vivo without apparent signs of toxicity.

SAE changes the histological structure of the tumor in lung cancer xenograft mice

The tumor histological changes in lung cancer xenograft mice were observed by optical microscopy after HE staining. The tumor cells were densely packed in the tissues of the control group (**Fig. 6**), but, were sparse in the tissues of the SAE-treated group. Marked mitotic activity and large blood vessels (yellow arrow) were observed in the control group. In contrast, the portions of cells in the SAE-treated group were necrotic, and inflammatory cells were observed around the tumor cell.

SAE suppresses STAT3 phosphorylation in lung cancer xenograft mice

After activation via phosphorylation, STAT3 modulates the expression of the key genes involved in regulating cell apoptosis, proliferation, and angiogenesis. This study examined the effect of SAE on the STAT3 phosphorylation level (p-STAT3) in tumor tissues. The IHC assay indicated that the SAE treatment had no effect on the changes in STAT3 expression but significantly suppressed the activation of the STAT3 pathway in lung cancer xenograft mice (**Fig. 7A**).

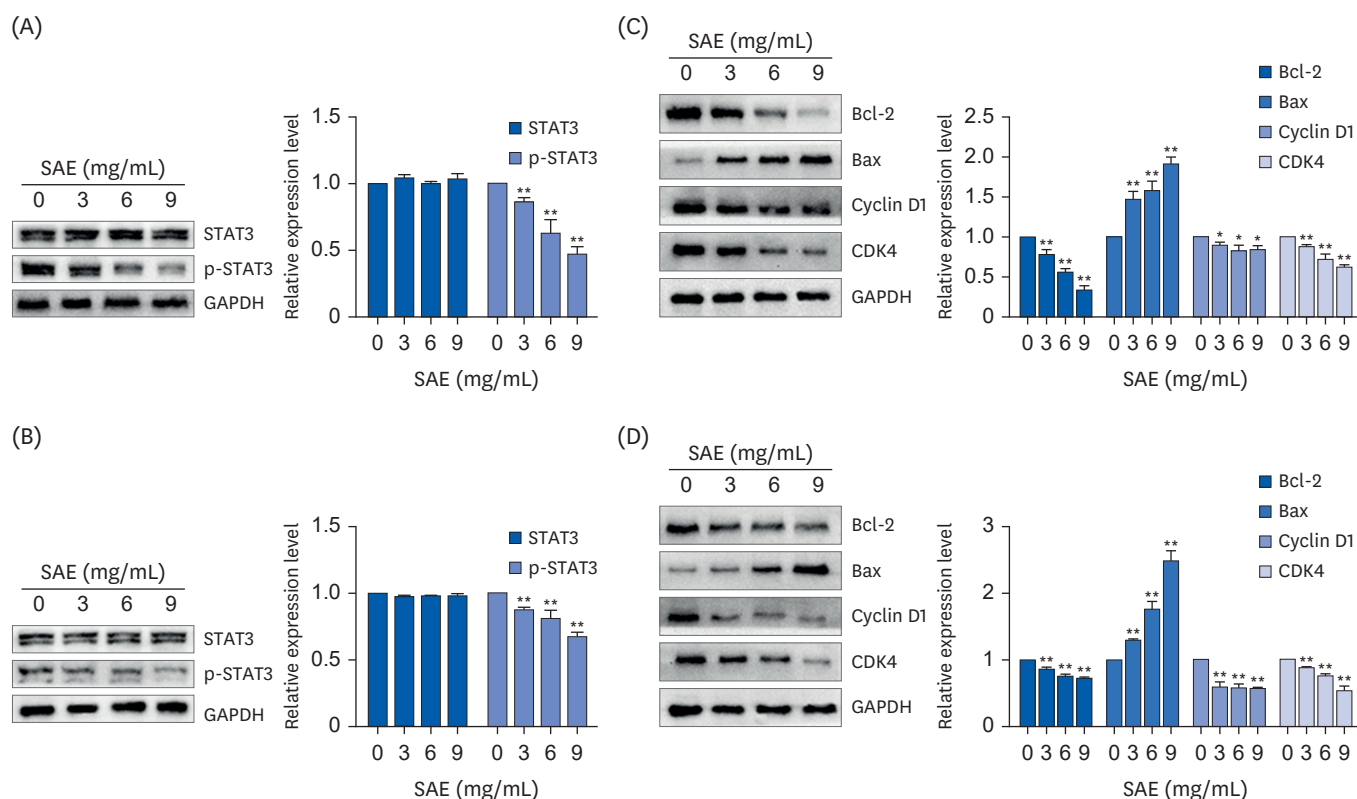


Fig. 4. SAE affect the protein expression of STAT3, Bcl-2, Bax, cyclin D1, and CDK4 in lung cancer cells. (A, B) The protein expression of STAT3 and p-STAT3 in A549 and H1650 were determined by western blotting. GAPDH was used as an internal control. (C, D) The protein levels of Bcl-2, Bax, cyclin D1 and CDK4 in A549 and H1650 treated by SAE were determined by western blotting. GAPDH was used as an internal control.

SAE, *Sanghuangporus sanghuang* alcohol extract; STAT3, signal transducer and activator of transcription 3; Bcl-2, B-cell lymphoma-2; Bax, Bcl2-associated X; CDK4, cyclin-dependent kinases 4; p-STAT3, phosphorylated signal transducer and activator of transcription 3; GAPDH, glyceraldehyde 3-phosphate dehydrogenase.

* $P < 0.05$, ** $P < 0.01$ vs. untreated control.

SAE regulates the expression of Bcl-2, Bax, cyclin D1, and CDK4 in lung cancer xenograft mice

The mechanism of the antitumor activity of SAE *in vivo* was examined by IHC analyses of the expression of Bcl-2, Bax, cyclin D1, and CDK4 proteins in lung cancer xenograft mice. The SAE treatment reduced the protein expression of pro-proliferative cyclin D1 and CDK4 and anti-apoptotic Bcl-2 in lung cancer xenografts, whereas that of proapoptotic Bax was increased significantly after the SAE treatment (Fig. 7B).

DISCUSSION

Tumorigenesis is strongly associated with the dysregulation of multiple biological processes and is influenced by many factors involving a range of aberrant genetic alterations [13]. Antitumor agents that target a single pathway might not always be effective in treating such a complex disease because of the complexity of cancer pathogenesis and progression [14]. Therefore, it plays an essential role in cancer treatment by targeting multiple tumor-promoting signaling pathways. Natural products, such as TCM, play a significant role in the prevention and treatment of cancer because of their low toxicity, low cost, and multiple targets [15].

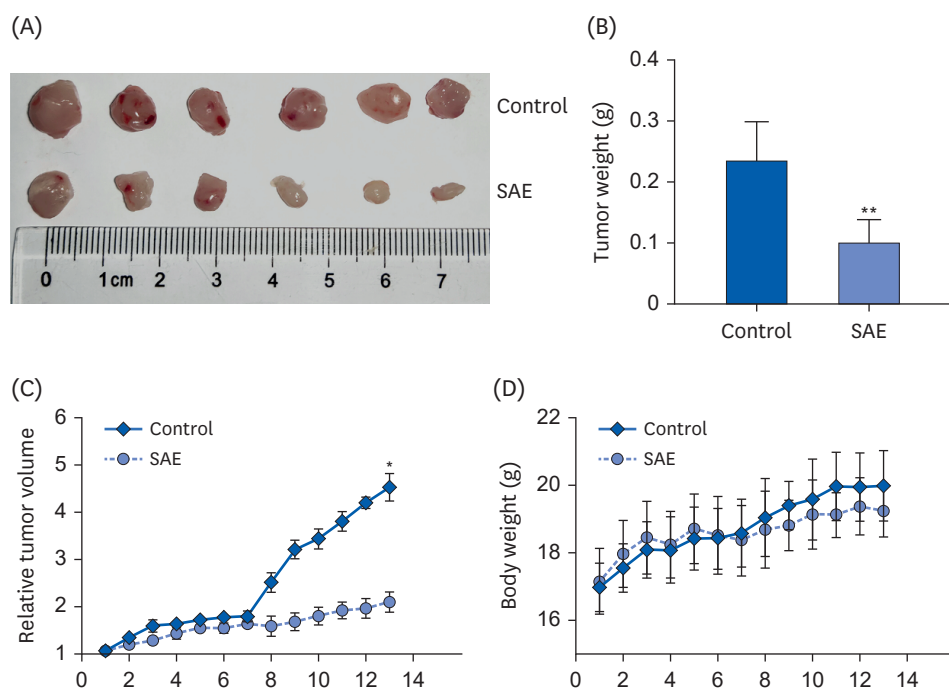


Fig. 5. SAE suppress the growth of subcutaneous tumor in mice. (A) The transplanted subcutaneous tumors. (B) Tumor weight of 2 groups. (C) Tumor volume changes in mice of 2 groups. (D) Body weight changes in mice of 2 groups. SAE, *Sanghuangporus sanghuang* alcohol extract. * $P < 0.05$, vs. control.

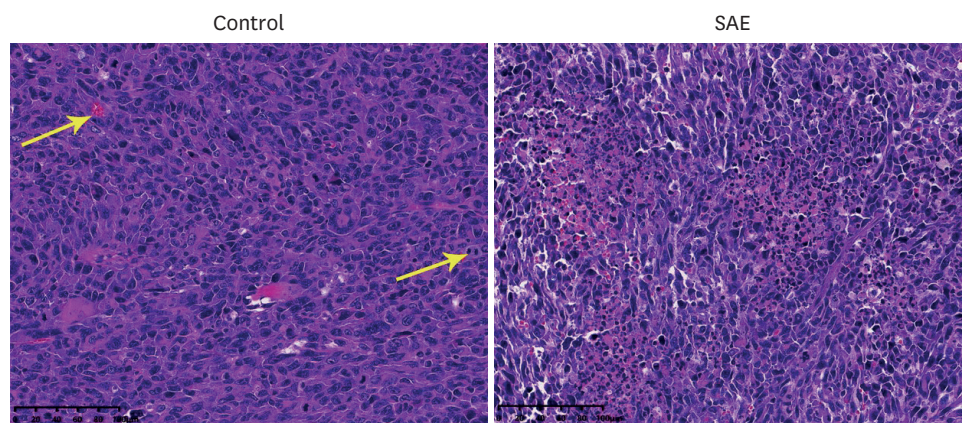


Fig. 6. Effect of SAE on the structural changes of tumor in lung cancer xenograft mice. Histopathological diversity were detected under a light microscope. Images are representative photographs taken at a magnification of 200 \times . SAE, *Sanghuangporus sanghuang* alcohol extract.

SS is considered one of the most effective anticancer traditional herbal resources in higher fungi and has been studied extensively as a medical remedy [16]. Previous studies showed that the sanghuang strain and its extract could suppress breast cancer cell growth and invasive by inhibiting AKT signaling [12]. The polysaccharides from sanghuang strains could inhibit human colon cancer cell proliferation and alter Wnt/ β -catenin signaling [17]. In addition, it also exerts synergistic antitumor effects in colorectal carcinoma by inhibiting the Reg IV/EGFR/Akt signaling pathway [18]. Nevertheless, the mechanism of its antitumor effects in lung cancer is still unclear.

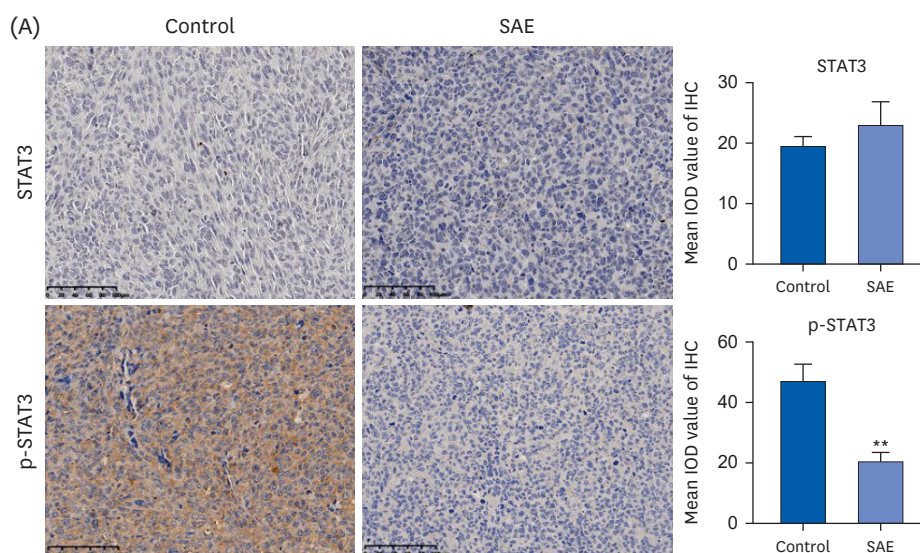


Fig. 7. Effect of SAE on the expression of Bcl-2, Bax, cyclin D1, CDK4, STAT3, and p-STAT3 in lung cancer xenograft mice. (A) SAE down-regulation of phosphorylation STAT3 in lung cancer xenograft mice. Total STAT3 and p-STAT3 were analyzed via immunohistochemical staining. The photographs are representative images taken at a magnification of 200 \times . (B) The protein expression levels of Bcl-2, Bax, cyclin D1, and CDK4 in tumor tissues were analyzed via immunohistochemical staining. The photographs are representative images taken at a magnification of 200 \times . SAE, *Sanghuangporus sanghuang* alcohol extract; Bcl-2, B-cell lymphoma-2; Bax, Bcl2-associated X; CDK4, cyclin-dependent kinases 4; STAT3, signal transducer and activator of transcription 3; p-STAT3, phosphorylated signal transducer and activator of transcription 3. * $P < 0.05$, ** $P < 0.01$ vs. control.

(continued to the next page)

The imbalance between cell proliferation and the cell death signals is the main characteristic of cancer. Therefore, inhibiting cell growth and inducing apoptosis may be the main strategy for cancer therapy [19]. This study found that SAE could remarkably inhibit the proliferation and DNA synthesis rate of A549 and H1650 cells in a dose and time-dependent manner. SAE reduced tumor weight significantly in A549 xenograft mice (a lung cancer mouse xenograft model), whereas it did not influence the change in body weight, suggesting that SAE suppressed lung cancer growth *in vivo* without causing additive toxicity.

The mitochondria play a crucial role in cell apoptosis. This process is regulated by Bcl-2 family proteins, such as Bcl-2 and Bax [20]. The Bcl-2/Bax balance is a critical factor determining the cell fate, and a change in the ratio of these proteins disrupts the normal apoptotic program, leading to numerous diseases, including cancer [21,22]. In malignant tumors, the ratio of Bcl-2/Bax is often increased, providing a survival advantage to the cancer cells and causing drug resistance [23]. Cyclin D1 and its catalytic partner CDK4 have been reported to play critical roles in the G1/S progression of the cell cycle. The cyclin D1/CDK4 complex is involved in controlling cell growth and prognostication in human malignant tumors [24]. The SAE treatment decreased the proapoptotic Bcl-2/Bax ratio *in vitro* and *in vivo*, suggesting that the changes in ratio might be involved in cell apoptosis. Furthermore, the data showed that the SAE treatment downregulated the expression of pro-proliferative proteins cyclin D1 and CDK4 *in vitro* and *in vivo*.

Tumor metastasis is a very complicated multistep action that plays an important role in cancer evolution and progression [25]. Migration and invasion are crucial cellular processes in cancer metastasis [26]. This study used scratch and transwell assays to evaluate the migratory and invasive ability of A549 and H1650 treated by SAE. SAE could significantly inhibit the metastasis and invasion of A549 and H1650 cells *in vitro* in a dose-dependent manner.

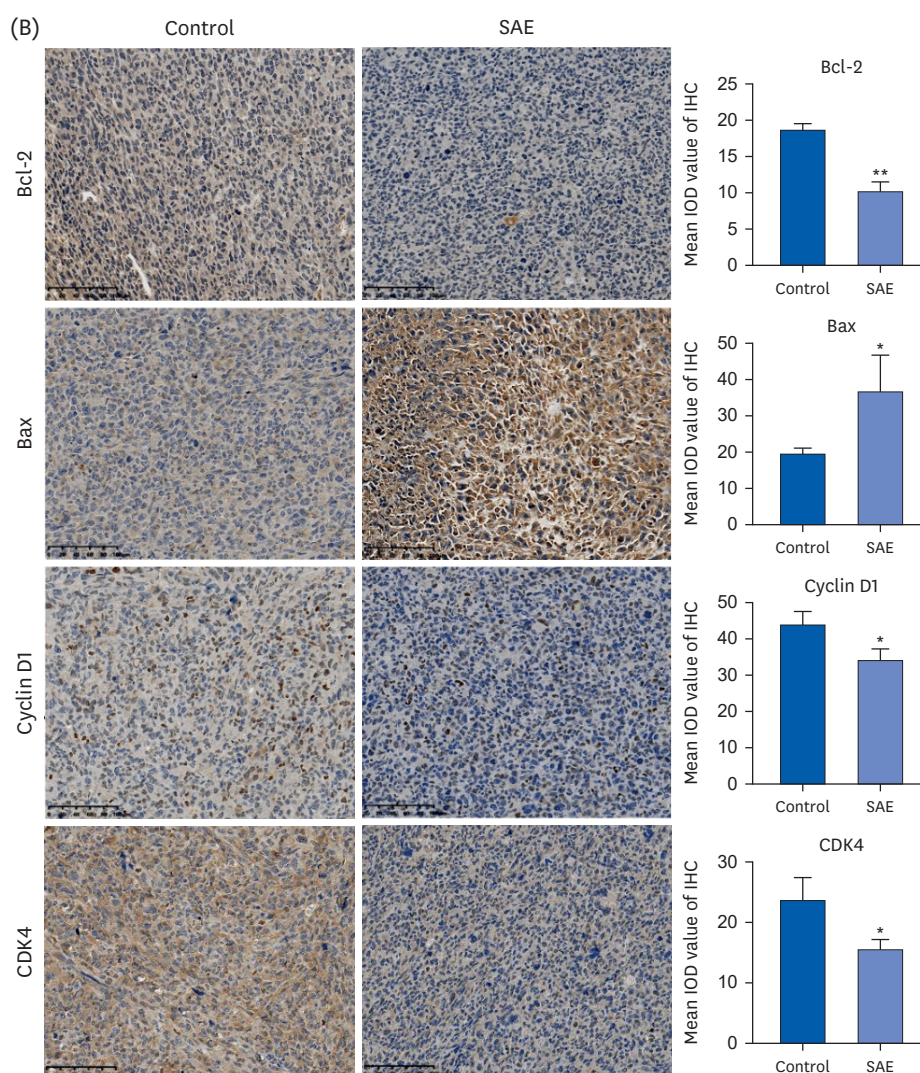


Fig. 7. (Continued) Effect of SAE on the expression of Bcl-2, Bax, cyclin D1, CDK4, STAT3, and p-STAT3 in lung cancer xenograft mice. (A) SAE down-regulation of phosphorylation STAT3 in lung cancer xenograft mice. Total STAT3 and p-STAT3 were analyzed via immunohistochemical staining. The photographs are representative images taken at a magnification of 200 \times . (B) The protein expression levels of Bcl-2, Bax, cyclin D1, and CDK4 in tumor tissues were analyzed via immunohistochemical staining. The photographs are representative images taken at a magnification of 200 \times . SAE, *Sanghuangporus sanghuang* alcohol extract; Bcl-2, B-cell lymphoma-2; Bax, Bcl2-associated X; CDK4, cyclin-dependent kinases 4; STAT3, signal transducer and activator of transcription 3; p-STAT3, phosphorylated signal transducer and activator of transcription 3. * $P < 0.05$, ** $P < 0.01$ vs. control.

STAT3 is a crucial cellular signaling involved in cancer development, including cancer cell proliferation, migration, invasion, and apoptosis [27]. In addition, it plays an important regulatory role in tumor occurrence and development. Therefore, STAT3 is a valuable target for cancer therapy [28]. A meta-analysis of the association between STAT3/p-STAT3 and breast cancer in China reported that STAT3/p-STAT3 expression plays a clinicopathological and prognostic role in diagnosis and treatment [29]. Therefore, inhibiting the constitutive STAT3 activity may be the most effective strategy for preventing and treating breast cancer. In this study, SAE could inhibit STAT3 phosphorylation both in vitro and in vivo, which might be related to the proapoptotic effect of SAE.

In conclusion, SAE reduced the cell viability and suppressed cell migration and invasion in human lung cancer cells. Moreover, the anti-proliferation effects of SAE observed in vitro

experiments could be translated to the *in vivo* situation, where remarkable effects on the tumor size can be observed. In addition, the results suggested that the antitumor effects of SAE are due partially to the inhibition of STAT3 signaling. These discoveries revealed the clinical application of SAE at molecular levels. The ethanolic extract from SS might be a valuable natural resource of antitumor agents, which may prompt cancer cell death and be a valuable additive to traditional chemotherapy. Nevertheless, further research is needed.

ACKNOWLEDGMENTS

The authors take thankful pleasure in acknowledging the unsparing assistance of all participants.

REFERENCES

1. Chen G, Zhang PG, Li JS, Duan JJ, Su W, Guo SP, Wang YF, Sun JN, Yang XT. Th17 cell frequency and IL-17A production in peripheral blood of patients with non-small-cell lung cancer. *J Int Med Res* 2020;48:300060520925948.
[PUBMED](#) | [CROSSREF](#)
2. Wang L, Wang W. Safety and efficacy of anaplastic lymphoma kinase tyrosine kinase inhibitors in non-small cell lung cancer (review) [Review]. *Oncol Rep* 2021;45:13-28.
[PUBMED](#) | [CROSSREF](#)
3. Ding Y, Lu Y, Xie X, Sheng B, Wang Z. Silencing TRIM37 inhibits the proliferation and migration of non-small cell lung cancer cells. *RSC Advances* 2018;8:36852-7.
[PUBMED](#) | [CROSSREF](#)
4. Wang Y, Ding Y, Zhao J, Wang C, Gao M, Chi X, Zhang B, Ma X, Li L. Dihydroartemisinin and doxorubicin co-loaded Soluplus®-TPGS mixed micelles: formulation characterization, cellular uptake, and pharmacodynamic studies. *Pharm Dev Technol* 2019;24:1125-32.
[PUBMED](#) | [CROSSREF](#)
5. Bukowski K, Kciuk M, Kontek R. Mechanisms of multidrug resistance in cancer chemotherapy. *Int J Mol Sci* 2020;21:3233-57.
[PUBMED](#) | [CROSSREF](#)
6. Hsiao WL, Liu L. The role of traditional Chinese herbal medicines in cancer therapy--from TCM theory to mechanistic insights. *Planta Med* 2010;76:1118-31.
[PUBMED](#) | [CROSSREF](#)
7. Dong J, Su SY, Wang MY, Zhan Z. Shenqi fuzheng, an injection concocted from Chinese medicinal herbs, combined with platinum-based chemotherapy for advanced non-small cell lung cancer: a systematic review. *J Exp Clin Cancer Res* 2010;29:137-48.
[PUBMED](#) | [CROSSREF](#)
8. Cai C, Ma J, Han C, Jin Y, Zhao G, He X. Extraction and antioxidant activity of total triterpenoids in the mycelium of a medicinal fungus, *Sanghuangporus sanghuang*. *Sci Rep* 2019;9:7418-28.
[PUBMED](#) | [CROSSREF](#)
9. Konno S, Chu K, Feuer N, Phillips J, Choudhury M. Potent anticancer effects of bioactive mushroom extracts (*Phellinus linteus*) on a variety of human cancer cells. *J Clin Med Res* 2015;7:76-82.
[PUBMED](#) | [CROSSREF](#)
10. Li G, Kim DH, Kim TD, Park BJ, Park HD, Park JI, Na MK, Kim HC, Hong ND, Lim K, et al. Protein-bound polysaccharide from *Phellinus linteus* induces G2/M phase arrest and apoptosis in SW480 human colon cancer cells. *Cancer Lett* 2004;216:175-81.
[PUBMED](#) | [CROSSREF](#)
11. Zhu T, Guo J, Collins L, Kelly J, Xiao ZJ, Kim SH, Chen CY. *Phellinus linteus* activates different pathways to induce apoptosis in prostate cancer cells. *Br J Cancer* 2007;96:583-90.
[PUBMED](#) | [CROSSREF](#)
12. Sliva D, Jedinak A, Kawasaki J, Harvey K, Slivova V. *Phellinus linteus* suppresses growth, angiogenesis and invasive behaviour of breast cancer cells through the inhibition of AKT signalling. *Br J Cancer* 2008;98:1348-56.
[PUBMED](#) | [CROSSREF](#)

13. Kiang KM, Leung GK. A review on adducin from functional to pathological mechanisms: future direction in cancer. *BioMed Res Int* 2018;2018:3465929.
[PUBMED](#) | [CROSSREF](#)
14. Lin W, Zheng L, Zhuang Q, Zhao J, Cao Z, Zeng J, Lin S, Xu W, Peng J. *Spica prunellae* promotes cancer cell apoptosis, inhibits cell proliferation and tumor angiogenesis in a mouse model of colorectal cancer via suppression of STAT3 pathway. *BMC Complement Altern Med* 2013;13:144-54.
[PUBMED](#) | [CROSSREF](#)
15. Chen Y, Wu H, Wang X, Wang C, Gan L, Zhu J, Tong J, Li Z. Huaier Granule extract inhibit the proliferation and metastasis of lung cancer cells through down-regulation of MTDH, JAK2/STAT3 and MAPK signaling pathways. *Biomed Pharmacother* 2018;101:311-21.
[PUBMED](#) | [CROSSREF](#)
16. Yan JK, Wang YY, Ma HL, Wang ZB. Ultrasonic effects on the degradation kinetics, preliminary characterization and antioxidant activities of polysaccharides from *Phellinus linteus* mycelia. *Ultrason Sonochem* 2016;29:251-7.
[PUBMED](#) | [CROSSREF](#)
17. Song KS, Li G, Kim JS, Jing K, Kim TD, Kim JP, Seo SB, Yoo JK, Park HD, Hwang BD, et al. Protein-bound polysaccharide from *Phellinus linteus* inhibits tumor growth, invasion, and angiogenesis and alters Wnt/ β -catenin in SW480 human colon cancer cells. *BMC Cancer* 2011;11:307-18.
[PUBMED](#) | [CROSSREF](#)
18. Li YG, Ji DF, Zhong S, Zhu JX, Chen S, Hu GY. Anti-tumor effects of proteoglycan from *Phellinus linteus* by immunomodulating and inhibiting Reg IV/EGFR/Akt signaling pathway in colorectal carcinoma. *Int J Biol Macromol* 2011;48:511-7.
[PUBMED](#) | [CROSSREF](#)
19. Reheman D, Zhao J, Guan S, Xu GC, Li YJ, Sun SR. Apoptotic effect of novel pyrazolone-based derivative [Cu(PMPP-SAL)(EtOH)] on HeLa cells and its mechanism. *Sci Rep* 2020;10:18235-47.
[PUBMED](#) | [CROSSREF](#)
20. Ramesh P, Medema JP. BCL-2 family deregulation in colorectal cancer: potential for BH3 mimetics in therapy. *Apoptosis* 2020;25:305-20.
[PUBMED](#) | [CROSSREF](#)
21. Cianfrocca R, Muscolini M, Marzano V, Annibaldi A, Marinari B, Levrero M, Costanzo A, Tuosto L. RelA/NF- κ B recruitment on the bax gene promoter antagonizes p73-dependent apoptosis in costimulated T cells. *Cell Death Differ* 2008;15:354-63.
[PUBMED](#) | [CROSSREF](#)
22. Bergandi L, Mungo E, Morone R, Bosco O, Rolando B, Doublier S. Hyperglycemia promotes chemoresistance through the reduction of the mitochondrial DNA damage, the Bax/Bcl-2 and Bax/Bcl-XL ratio, and the cells in sub-G1 phase due to antitumoral drugs induced-cytotoxicity in human colon adenocarcinoma cells. *Front Pharmacol* 2018;9:866-89.
[PUBMED](#) | [CROSSREF](#)
23. Youle RJ, Strasser A. The BCL-2 protein family: opposing activities that mediate cell death. *Nat Rev Mol Cell Biol* 2008;9:47-59.
[PUBMED](#) | [CROSSREF](#)
24. Dong Y, Sui L, Sugimoto K, Tai Y, Tokuda M. Cyclin D1-CDK4 complex, a possible critical factor for cell proliferation and prognosis in laryngeal squamous cell carcinomas. *Int J Cancer* 2001;95:209-15.
[PUBMED](#) | [CROSSREF](#)
25. Testa U, Pelosi E, Castelli G. Colorectal cancer: genetic abnormalities, tumor progression, tumor heterogeneity, clonal evolution and tumor-initiating cells. *Med Sci (Basel)* 2018;6:31-144.
[PUBMED](#) | [CROSSREF](#)
26. Friedl P, Wolf K. Tumour-cell invasion and migration: diversity and escape mechanisms. *Nat Rev Cancer* 2003;3:362-74.
[PUBMED](#) | [CROSSREF](#)
27. Yu H, Lee H, Herrmann A, Buettner R, Jove R. Revisiting STAT3 signalling in cancer: new and unexpected biological functions. *Nat Rev Cancer* 2014;14:736-46.
[PUBMED](#) | [CROSSREF](#)
28. Chai EZ, Shanmugam MK, Arfuso F, Dharmarajan A, Wang C, Kumar AP, Samy RP, Lim LH, Wang L, Goh BC, et al. Targeting transcription factor STAT3 for cancer prevention and therapy. *Pharmacol Ther* 2016;162:86-97.
[PUBMED](#) | [CROSSREF](#)
29. Li Y, Wang Y, Shi Z, Liu J, Zheng S, Yang J, Liu Y, Yang Y, Chang F, Yu W. Clinicopathological and prognostic role of STAT3/p-STAT3 in breast cancer patients in China: a meta-analysis. *Sci Rep* 2019;9:11243-52.
[PUBMED](#) | [CROSSREF](#)